



## Supplementary Information for

A carbonate-rich lake solution to the phosphate problem of the origin of life

Jonathan D. Toner and David C. Catling

Jonathan D. Toner

Email: [toner2@uw.edu](mailto:toner2@uw.edu)

### **This PDF file includes:**

- Appendix A: The composition of carbonate-rich lakes
- Appendix B: Results of experiments on gypsum addition to phosphate-rich brines
- Appendix C: Geochemical models
- Figs. S1 to S6
- Tables S1 to S2
- References for SI reference citations

## Supplementary Material

### Appendix A: The composition of carbonate-rich lakes

Carbonate-rich lakes accumulate a number of ions, in addition to phosphate, from their hydrologic basins, and concentrate these ions until they precipitate from solution as salts (1) (Fig. S1). Most ion concentrations in carbonate-rich lakes, with the exception of  $\text{Ca}^{2+}$  and  $\text{Mg}^{2+}$ , increase linearly with phosphate in approximately 1:1 trends (Fig. S1). This indicates that phosphate in carbonate-rich lakes behaves as a conservative solute, that is, it does not precipitate during evaporation as a salt. This is in stark contrast to the situation in most surface waters on Earth, where phosphate has a highly non-conservative behavior and precipitates as apatite minerals.

The conservative behavior of phosphate is best appreciated in relation to  $\text{Br}^-$ , one of the most conservative ions in carbonate-rich lake brines because it forms highly soluble salts and does not significantly coprecipitate with other halides. In general, phosphate varies with  $\text{Br}^-$  along a 1:1 trend (the dashed line in the  $\text{Br}^-$  vs. phosphate plot in Fig. S1), which indicates that phosphate also behaves as a conservative ion. Other ions, such as  $\text{Cl}^-$  and  $\text{Na}^+$ , are also highly conservative and show a similar trend with phosphate.

The highest concentration ions in carbonate-rich lakes are invariably  $\text{Na}^+$  and  $\text{Cl}^-$ . Sodium ion concentrations reach up to ~9 molal, at which point  $\text{Na}^+$  precipitates as highly soluble  $\text{NaCl}$  and  $\text{NaHCO}_3/\text{Na}_2\text{CO}_3$  phases. Similarly,  $\text{Cl}^-$  concentrations up to ~6 molal are possible before the  $\text{Cl}^-$  precipitates as halite ( $\text{NaCl}$ ). In modern carbonate-rich lakes, phosphate concentrations above ~1  $\text{mmol}\cdot\text{kg}^{-1}$  commonly occur in brines saturated with respect to  $\text{NaCl}$  and  $\text{NaHCO}_3/\text{Na}_2\text{CO}_3$  salts.  $\text{K}^+$  ions have a similar chemistry to  $\text{Na}^+$ , but on average the  $\text{K}^+/\text{Na}^+$  ratio in carbonate-rich lakes is ~0.05, and the highest concentrations are ~1 molal. Lower  $\text{K}^+$  relative to  $\text{Na}^+$  is caused by several factors. First,  $\text{K}^+$  salts such as arcanite ( $\text{K}_2\text{SO}_4$ ) and sylvite ( $\text{KCl}$ ) are less soluble than their  $\text{Na}^+$  analogs. Second,  $\text{K}^+$  ions undergo irreversible ion exchange fixation and precipitates in secondary silicate minerals (1).

Other ions that have appreciable concentrations in carbonate-rich brines are boron species and  $\text{SO}_4^{2-}$ . Boron concentrations are especially high in Searles Lake (~0.4 molal) (2), although Owens lake in California also attains high boron concentrations during evaporation (3). Boron concentrations are limited by highly soluble borax salts ( $\text{Na}_2\text{B}_4\text{O}_7\cdot 10\text{H}_2\text{O}$ ) (4). On present-day Earth, boron derives from weathering of boron-enriched continental crust (5). Although less land was likely present at life's origin than today, trace boron could have accumulated in significant concentrations via evaporative concentration in closed-basin lakes even on small amounts of land, such as ocean islands. Finally,  $\text{SO}_4^{2-}$  reaches concentrations of ~1 molal before precipitating as  $\text{Na}^+$  and  $\text{K}^+$  salts such as mirabillite ( $\text{Na}_2\text{SO}_4\cdot 10\text{H}_2\text{O}$ ), arcanite, and thenardite ( $\text{Na}_2\text{SO}_4$ ).

$\text{Ca}^{2+}$  and  $\text{Mg}^{2+}$  ions generally have relatively low concentrations in carbonate-rich lakes, as expected based on high concentrations of carbonate ions. In some cases,  $\text{Ca}^{2+}$  and  $\text{Mg}^{2+}$  attain maximum concentrations of ~10 mM in carbonate-rich lakes; however, we question the accuracy of such high literature values. Almost all of the high  $\text{Ca}^{2+}$  values in Fig. S1 corresponding to high phosphate concentrations are from a single study (6). This study measured  $\text{Ca}^{2+}$  and  $\text{Mg}^{2+}$  using

Inductively Coupled Optical Emission Spectroscopy (ICP-OES); however, ICP-OES suffers from matrix effects when measuring trace components in concentrated solutions, which may raise the apparent ion concentration. Given that Ref. (6) gives little information on the analytical procedure, and that the  $\text{Ca}^{2+}$  and  $\text{Mg}^{2+}$  values are anomalously high, these measurements are of questionable accuracy. Other anomalously high  $\text{Ca}^{2+}$  values are from analyses done prior to ~1920, and so are also of questionable accuracy.

As an example of possible inaccuracies in literature  $\text{Ca}^{2+}$  analyses, Owens Lake, California, was analyzed prior to ~1920 and found to have ~1 mM  $\text{Ca}^{2+}$  (7). In comparison, a later study done by highly competent researchers measured 0.05-0.2 mM  $\text{Ca}^{2+}$  (3), which decrease with increasing carbonate alkalinity during evaporation as expected. We may also compare environmental  $\text{Ca}^{2+}$  concentrations with careful laboratory measurements of calcite solubility in  $\text{Na}_2\text{CO}_3$  solutions (8), which indicate  $\text{Ca}^{2+}$  concentrations between 0.01-0.1 mM  $\text{Ca}^{2+}$  depending on the inorganic carbon concentration. Furthermore, we measured  $\text{Ca}^{2+}$  concentrations in several of the experimental brines in this manuscript (see SI Appendix B), and found that concentrations are ~0.1 mM.

Carbonate-rich lakes are rich in many other ions such as  $\text{F}^-$ ,  $\text{Li}^+$ , silica, and trace metals (9-11). In particular, silica and trace metals accumulate because of the formation of more soluble ion complexes in the presence of high pH and/or high concentrations of background ions. Silica accumulates at relatively high concentrations in carbonate-rich lakes because  $\text{H}_3\text{SiO}_4^-$  and  $\text{H}_2\text{SiO}_4^{2-}$  species form at high pH, instead of  $\text{H}_4\text{SiO}_4^0$  species at low pH. Similarly, trace metals are relatively soluble in carbonate-rich lakes because they form complexes with concentrated  $\text{Cl}^-$ ,  $\text{OH}^-$ ,  $\text{HCO}_3^-$ , and  $\text{CO}_3^{2-}$  ions.

Finally, we note that phosphorus may be present in inorganic and organic forms. In most analyses presented in Fig. S1, phosphate is measured using colorimetric methods, which is sensitive only to dissolved inorganic phosphate; however, measurements of the bulk P content by atomic emission methods yields only the total dissolved P (inorganic + organic phosphorus). In these cases (e.g., the P analyses for Goodenough and Last Chance lakes), a fraction of the total measured dissolved P may be due to the dissolved organic phosphorus.

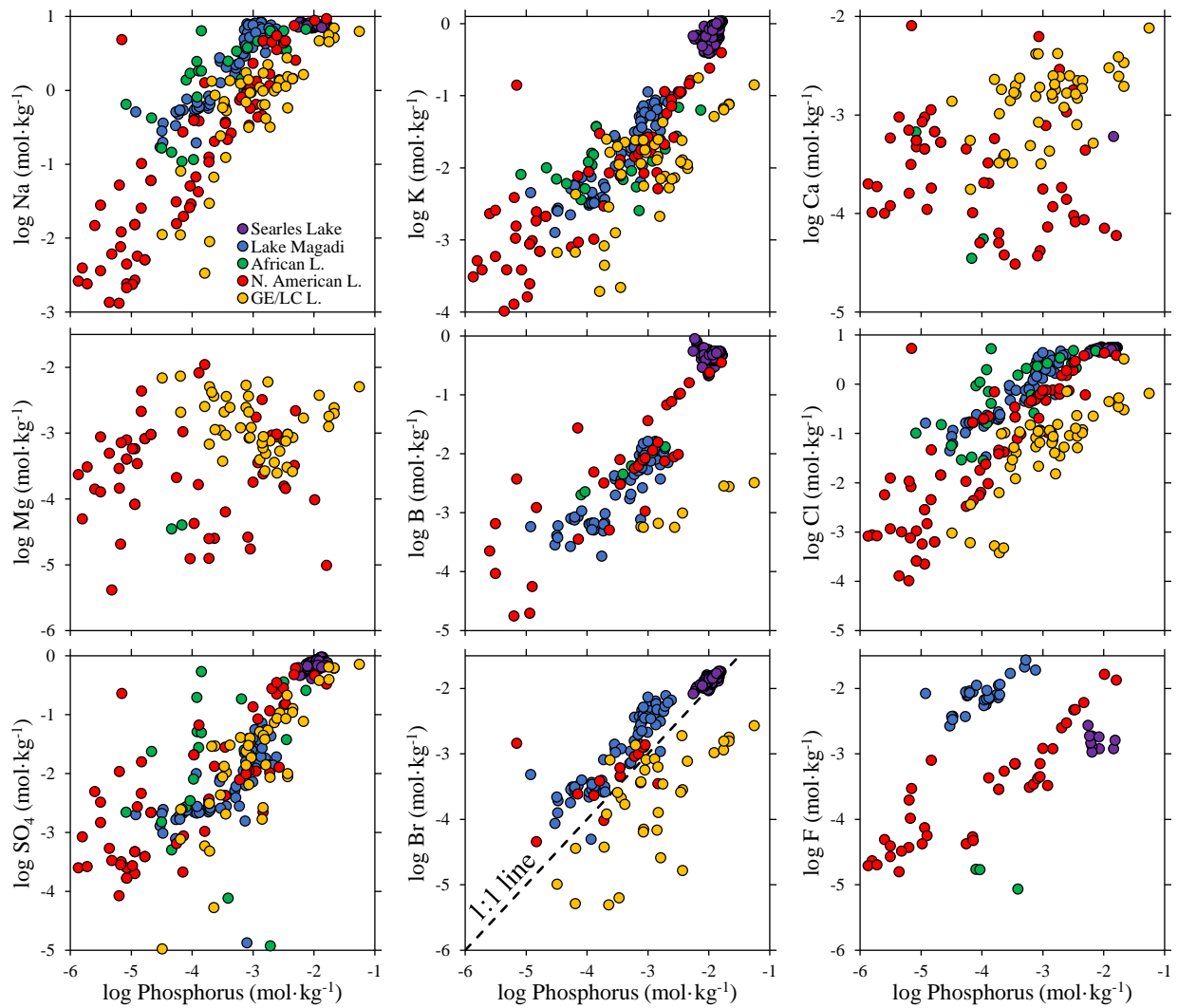


Fig. S1. Concentrations of P, Na<sup>+</sup>, K<sup>+</sup>, Ca<sup>2+</sup>, Mg<sup>2+</sup>, B, Cl<sup>-</sup>, SO<sub>4</sub><sup>2-</sup>, Br<sup>-</sup>, and F<sup>-</sup> in Searles Lake, Lake Magadi, Goodenough and Last Chance lakes (GE/LC L.), various other African lakes (African L.), and various other North American Lakes (N. American L.). We only plot lake compositions that have been analyzed for phosphate/phosphorus. The dashed line in the Br<sup>-</sup> vs. phosphorus plot indicates the 1:1 trend expected for conservative solutes.

## Appendix B: Results of experiments on gypsum addition to phosphate-rich brines

The results of our experiments on phosphate- and carbonate-rich brines in the lab are presented here. Table S1 describes the initial salt content of the solutions, the salt concentration after equilibration (calculated by accounting for ions precipitated in solid phases, as described in the *Methods* section), and the modeled pH, pCO<sub>2</sub>, and %HCO<sub>3</sub> in the equilibrated solution. Table S2 describes the composition of solid phases on a dry weight basis after equilibration, where the CO<sub>3</sub><sup>2-</sup> content is calculated based on charge balance (as described in the *Methods* section). Finally, the XRD profiles of the solid phases listed in Table S2 are presented in Fig. S2 through Fig. S6.

To check our modeled pH values listed in Table S1, we also measured the pH of several solutions with a standard glass electrode, and found that the measured pH was typically within 0.2 of the modeled value. We note that pH measurements in salt solutions are complicated by several sources of error, such as theoretical uncertainties on the value of single ion activity coefficients in concentrated solutions and liquid junction potential errors (12). Another possible issue is that the modeled pH is sensitive to errors in the composition of the precipitated salts, which we subtract from the initial prepared solution composition to arrive at the final solution composition. First, measured ion concentrations have likely errors of approximately ±5 % based on the accuracy of ICP-OES analyses. Second, errors in the assumed ionic speciation of the solid phases can affect the modeled pH. For precipitated solids, we assumed that only CO<sub>3</sub><sup>2-</sup> and PO<sub>4</sub><sup>3-</sup> ions were present, based on solids identified via XRD, but HCO<sub>3</sub><sup>-</sup> and HPO<sub>4</sub><sup>2-</sup> ions may also have been present in the solids. Removing CO<sub>3</sub><sup>2-</sup> and PO<sub>4</sub><sup>3-</sup> ions from the initial solution results in a lower modeled pH than if HCO<sub>3</sub><sup>-</sup> and HPO<sub>4</sub><sup>2-</sup> ions are removed. This is because CO<sub>3</sub><sup>2-</sup> and PO<sub>4</sub><sup>3-</sup> ions have more alkalinity than equivalent concentrations of HCO<sub>3</sub><sup>-</sup> and HPO<sub>4</sub><sup>2-</sup> ions.

Another key assumption in our analysis is that all of the Ca<sup>2+</sup> in the experimental solutions remained in solid phases. We tested this by measuring Ca<sup>2+</sup> in a representative suite of four samples using ICP-OES (sample numbers 1, 8, 9, and 11 in Table S1). To achieve the highest possible accuracy, we corrected for matrix effects by spiking each sample with known amounts of Ca<sup>2+</sup>, and ensuring that no precipitates formed by acidifying with HNO<sub>3</sub>. Each sample was analyzed with no added Ca<sup>2+</sup>, followed by three replicate samples with increasing amounts of Ca<sup>2+</sup>. We then calculate the Ca<sup>2+</sup> in the unspiked samples by linear regression of the spiked samples. The lowest concentration of Ca<sup>2+</sup> that we spiked the samples with was 0.1 mmol·kg<sup>-1</sup>. Our results indicate that Ca<sup>2+</sup> concentrations are 0.07, 0.11, 0.045, and 0.033 mmol·kg<sup>-1</sup> for sample numbers 1, 8, 9, and 11 respectively in Table S1. For an initial added Ca<sup>2+</sup> concentration of 100 mmol·kg<sup>-1</sup>, this means that ~99.9 % of the added Ca<sup>2+</sup> remained in solid phases over the course of the experiment.

Table S1. The concentration of ions (molal) in the initial and final solutions equilibrated over 1 to 4 weeks. The initial total molality is the molality of all salts initially added to the experiment, including gypsum. The final aqueous molality is the solution molality after equilibration, which is calculated by assuming all  $\text{Ca}^{2+}$  is present in solid phases, and subtracting ions precipitated in solid phases (see Table S2) from the initial total molality. Finally, the modeled values for the equilibrated solution were determined by modeling gas-solution equilibrium with 100 ml of headspace (as in the experimental set-up) using the geochemical program PHREEQC and the aqueous database THEREDA.

| #   | Time weeks | Initial Total Molality |       |                 |      |       |       | Final Aqueous Molality |                 |      |       | Modeled Aqueous Values |       |  |                   |
|---|------------|------------------------|-------|-----------------|------|-------|-------|------------------------|-----------------|------|-------|------------------------|-------|--|-------------------|
|   |            | Na                     | Ca    | SO <sub>4</sub> | C    | P     | F     | Na                     | SO <sub>4</sub> | C    | P     | F                      | pH    | log <sub>10</sub> (pCO <sub>2</sub> ) bars | %HCO <sub>3</sub> |
| <i>Series 1: Variable HCO<sub>3</sub>:CO<sub>2</sub> ratio, with and without fluoride</i> |            |                        |       |                 |      |       |       |                        |                 |      |       |                        |       |  |                   |
| 1   | 2          | 1.19                   | 0.099 | 0.099           | 1.09 | 0.049 |       | 1.17                   | 0.099           | 1.04 | 0.014 |                        | 7.03  | 0.48                                       | 99.4              |
| 2   | 2          | 1.2                    | 0.099 | 0.099           | 1.09 | 0.049 |       | 1.19                   | 0.099           | 1.04 | 0.011 |                        | 7.11  | 0.41                                       | 99.3              |
| 3   | 2          | 1.21                   | 0.099 | 0.099           | 1.09 | 0.049 |       | 1.2                    | 0.099           | 1.03 | 0.021 |                        | 7.16  | 0.36                                       | 99.2              |
| 4   | 2          | 1.23                   | 0.099 | 0.099           | 1.09 | 0.049 |       | 1.23                   | 0.099           | 1.03 | 0.021 |                        | 7.3   | 0.22                                       | 98.9              |
| 5   | 2          | 1.26                   | 0.099 | 0.099           | 1.09 | 0.049 |       | 1.25                   | 0.099           | 1.03 | 0.025 |                        | 7.49  | 0.04                                       | 98.3              |
| 6   | 2          | 1.28                   | 0.099 | 0.099           | 1.09 | 0.049 |       | 1.27                   | 0.099           | 1.01 | 0.033 |                        | 7.71  | -0.19                                      | 97.2              |
| 7   | 2          | 1.65                   | 0.099 | 0.099           | 1.29 | 0.049 |       | 1.64                   | 0.099           | 1.19 | 0.049 |                        | 8.67  | -1.17                                      | 76.4              |
| 8   | 2          | 2.32                   | 0.099 | 0.099           | 1.59 | 0.049 |       | 2.26                   | 0.099           | 1.46 | 0.048 |                        | 9.11  | -1.72                                      | 48.6              |
| 9   | 2          | 3.43                   | 0.099 | 0.099           | 2.08 | 0.049 |       | 3.23                   | 0.099           | 1.88 | 0.048 |                        | 9.39  | -2.13                                      | 28.5              |
| 10  | 2          | 5.46                   | 0.099 | 0.099           | 2.98 | 0.049 |       | 5.31                   | 0.099           | 2.81 | 0.049 |                        | 9.78  | -2.73                                      | 12                |
| 11  | 2          | 5.06                   | 0.099 | 0.099           | 2.48 | 0.049 |       | 4.91                   | 0.099           | 2.31 | 0.048 |                        | 11.05 | -5.25                                      | 0.8               |
| 12  | 2          | 1.04                   | 0.05  | 0.05            | 0.93 | 0.05  | 0.009 | 1.03                   | 0.05            | 0.92 | 0.025 | 0.009                  | 7.44  | 0.05                                       | 98.6              |
| 13  | 2          | 1.21                   | 0.05  | 0.05            | 1.1  | 0.05  | 0.009 | 1.21                   | 0.05            | 1.08 | 0.027 | 0.009                  | 7.56  | 0  | 98.1              |
| 14  | 2          | 1.23                   | 0.05  | 0.05            | 1.1  | 0.05  | 0.009 | 1.22                   | 0.05            | 1.08 | 0.028 | 0.009                  | 7.68  | -0.12                                      | 97.5              |
| 15  | 2          | 1.25                   | 0.05  | 0.05            | 1.1  | 0.05  | 0.009 | 1.24                   | 0.05            | 1.07 | 0.034 | 0.009                  | 7.9   | -0.35                                      | 95.8              |
| 16  | 2          | 1.27                   | 0.05  | 0.05            | 1.1  | 0.05  | 0.009 | 1.27                   | 0.05            | 1.06 | 0.036 | 0.009                  | 8.13  | -0.59                                      | 93                |
| 17  | 2          | 1.29                   | 0.05  | 0.05            | 1.1  | 0.05  | 0.009 | 1.29                   | 0.05            | 1.06 | 0.037 | 0.009                  | 8.3   | -0.78                                      | 89.8              |
| 18  | 2          | 1.43                   | 0.05  | 0.05            | 1.1  | 0.05  | 0.009 | 1.43                   | 0.05            | 1.05 | 0.049 | 0.009                  | 8.83  | -1.4                                       | 70.7              |
| 19  | 2          | 2.01                   | 0.05  | 0.05            | 1.36 | 0.05  | 0.009 | 2                      | 0.05            | 1.3  | 0.049 | 0.009                  | 9.21  | -1.89                                      | 44.6              |
| 20  | 2          | 2.95                   | 0.05  | 0.05            | 1.78 | 0.05  | 0.009 | 2.92                   | 0.05            | 1.71 | 0.05  | 0.009                  | 9.48  | -2.29                                      | 25.9              |
| 21  | 2          | 4.68                   | 0.05  | 0.05            | 2.54 | 0.05  | 0.009 | 4.64                   | 0.05            | 2.47 | 0.049 | 0.009                  | 9.83  | -2.85                                      | 11.4              |
| 22  | 2          | 4.34                   | 0.05  | 0.05            | 2.12 | 0.05  | 0.009 | 4.28                   | 0.05            | 2.04 | 0.049 | 0.009                  | 11.13 | -5.45                                      | 0.7               |
| <i>Series 2: Variable equilibration time, without fluoride</i>                            |            |                        |       |                 |      |       |       |                        |                 |      |       |                        |       |  |                   |
| 23  | 1          | 2.33                   | 0.099 | 0.099           | 1.59 | 0.049 |       | 2.2                    | 0.099           | 1.43 | 0.048 |                        | 9.09  | -1.69                                      | 50.3              |
| 24  | 2          | 2.33                   | 0.1   | 0.1             | 1.59 | 0.05  |       | 2.27                   | 0.099           | 1.47 | 0.049 |                        | 9.11  | -1.72                                      | 48.6              |
| 25  | 3          | 2.32                   | 0.099 | 0.099           | 1.59 | 0.049 |       | 2.32                   | 0.099           | 1.49 | 0.049 |                        | 9.13  | -1.74                                      | 47.2              |
| 26  | 4          | 2.32                   | 0.099 | 0.099           | 1.59 | 0.049 |       | 2.32                   | 0.099           | 1.49 | 0.049 |                        | 9.13  | -1.74                                      | 47.2              |
| <i>Series 3: Variable initial phosphate concentration, with and without fluoride</i>      |            |                        |       |                 |      |       |       |                        |                 |      |       |                        |       |  |                   |
| 27  | 2          | 2.07                   | 0.099 | 0.099           | 1.34 | 0.099 |       | 2.06                   | 0.099           | 1.24 | 0.098 |                        | 9.13  | -1.8                                       | 48.8              |
| 28  | 2          | 2.26                   | 0.099 | 0.099           | 1.34 | 0.199 |       | 2.2                    | 0.099           | 1.28 | 0.148 |                        | 9.08  | -1.73                                      | 50.7              |
| 29  | 2          | 2.46                   | 0.099 | 0.099           | 1.34 | 0.298 |       | 2.39                   | 0.099           | 1.29 | 0.243 |                        | 9.05  | -1.71                                      | 50.9              |
| 30  | 2          | 2.66                   | 0.099 | 0.099           | 1.34 | 0.397 |       | 2.59                   | 0.099           | 1.29 | 0.339 |                        | 9.03  | -1.7                                       | 51                |
| 31  | 2          | 2.86                   | 0.099 | 0.099           | 1.34 | 0.497 |       | 2.8                    | 0.099           | 1.3  | 0.436 |                        | 9.01  | -1.68                                      | 50.9              |
| 32  | 2          | 1.93                   | 0.05  | 0.05            | 1.36 | 0.01  | 0.009 | 1.92                   | 0.05            | 1.3  | 0.01  | 0.009                  | 9.22  | -1.9                                       | 44.5              |
| 33  | 2          | 1.95                   | 0.05  | 0.05            | 1.36 | 0.02  | 0.009 | 1.94                   | 0.05            | 1.3  | 0.02  | 0.009                  | 9.22  | -1.9                                       | 44.5              |
| 34  | 2          | 2.01                   | 0.05  | 0.05            | 1.36 | 0.05  | 0.009 | 2                      | 0.05            | 1.3  | 0.05  | 0.009                  | 9.21  | -1.89                                      | 44.6              |
| 35  | 2          | 2.1                    | 0.05  | 0.05            | 1.36 | 0.099 | 0.009 | 2.1                    | 0.05            | 1.31 | 0.096 | 0.009                  | 9.2   | -1.88                                      | 44.7              |
| 36  | 2          | 2.3                    | 0.05  | 0.05            | 1.36 | 0.198 | 0.009 | 2.29                   | 0.05            | 1.33 | 0.182 | 0.009                  | 9.16  | -1.85                                      | 45.1              |

Table S2. The concentration of ions (wt. %) in solid phases after equilibration of the solutions given in Table S1, and drying at 60°C in a vacuum oven overnight. Na, Ca, P, and S were measured using inductively coupled optical emission spectroscopy (ICP-OES), whereas the  $\text{CO}_3^{2-}$  content was calculated via charge balance (see Methods). Phases determined via XRD analysis (presented in Fig. S2 through Fig. S6) are given in the last column.

| #   | Na    | Ca    | PO <sub>4</sub> | SO <sub>4</sub> | CO <sub>3</sub> | Total  | XRD Phases          |
|---|-------|-------|-----------------|-----------------|-----------------|--------|---------------------|
| wt. %   |       |       |                 |                 |                 |        |                     |
| <i>Series 1: Variable HCO<sub>3</sub>:CO<sub>3</sub> ratio, with and without fluoride</i> |       |       |                 |                 |                 |        |                     |
| 1   | 3.46  | 33.34 | 28.66           | 0.77            | 26.88           | 93.12  | calcite, apatite    |
| 2   | 2.52  | 37.7  | 34.88           | 0.06            | 26.75           | 101.91 | calcite, apatite    |
| 3   | 1.81  | 38.12 | 26.02           | 0.46            | 34.59           | 101    | calcite, apatite    |
| 4   | 2.08  | 37.47 | 25.31           | 0.3             | 34.75           | 99.91  | calcite, apatite    |
| 5   | 1.82  | 36.93 | 21.42           | 0.22            | 37.34           | 97.73  | calcite, apatite    |
| 6   | 1.37  | 37.99 | 15.08           | 0.25            | 44.33           | 99.01  | calcite, apatite    |
| 7   | 0.79  | 39.09 | 0.85            | 0.13            | 58.78           | 99.65  | calcite             |
| 8   | 9.68  | 27.25 | 0.62            | 0.14            | 52.83           | 90.53  | calcite, gaylussite |
| 9   | 20.25 | 17.07 | 0.42            | 0.15            | 51.53           | 89.41  | calcite, gaylussite |
| 10  | 18.26 | 20.95 | 0.42            | 0.34            | 54.64           | 94.61  | calcite, gaylussite |
| 11  | 18.47 | 20.63 | 0.54            | 0.4             | 54.28           | 94.31  | calcite, gaylussite |
| 12  | 2.61  | 36.98 | 43.1            | 0               | 18.03           | 100.72 | apatite             |
| 13  | 2.91  | 35.84 | 38.6            | 0.09            | 20.93           | 98.36  | calcite, apatite    |
| 14  | 2.84  | 36.9  | 38.56           | 0.1             | 22.45           | 100.86 | calcite, apatite    |
| 15  | 2.75  | 37.31 | 28.55           | 0.2             | 32.37           | 101.17 | calcite, apatite    |
| 16  | 2.18  | 38.47 | 24.8            | 0.1             | 36.99           | 102.53 | calcite, apatite    |
| 17  | 2.12  | 38.03 | 22.32           | 0               | 38.67           | 101.14 | calcite, apatite    |
| 18  | 0.53  | 39.68 | 0.98            | 0               | 59.29           | 100.49 | calcite             |
| 19  | 0.65  | 39.98 | 0.21            | 0               | 60.62           | 101.45 | calcite             |
| 20  | 12.07 | 27.46 | 0.08            | 0               | 56.86           | 96.47  | calcite, gaylussite |
| 21  | 14.33 | 26.47 | 0.21            | 0.1             | 58.14           | 99.25  | calcite, gaylussite |
| 22  | 17.8  | 23.06 | 0.68            | 0.09            | 57.12           | 98.75  | calcite, gaylussite |
| <i>Series 2: Variable equilibration time, without fluoride</i>                            |       |       |                 |                 |                 |        |                     |
| 23  | 16.37 | 22.17 | 0.7             | 0.2             | 53.83           | 93.28  | calcite, gaylussite |
| 24  | 9.68  | 27.25 | 0.62            | 0.14            | 52.83           | 90.53  | calcite, gaylussite |
| 25  | 1.06  | 39.52 | 0.57            | 0.08            | 60.08           | 101.31 | calcite             |
| 26  | 0.96  | 38.82 | 0.69            | 0.08            | 58.78           | 99.33  | calcite             |
| <i>Series 3: Variable initial phosphate concentration, with and without fluoride</i>      |       |       |                 |                 |                 |        |                     |
| 27  | 1.13  | 38.57 | 1.07            | 0.11            | 58.25           | 99.13  | Ca-Na phosphate     |
| 28  | 10.13 | 27.13 | 33.02           | 0.32            | 22.42           | 93.02  | Ca-Na phosphate     |
| 29  | 10.99 | 27.63 | 36.33           | 0.41            | 21.09           | 96.45  | Ca-Na phosphate     |
| 30  | 11.02 | 27.11 | 37.84           | 0.58            | 18.82           | 95.37  | Ca-Na phosphate     |
| 31  | 10.31 | 28.04 | 40.47           | 0.5             | 16.85           | 96.16  | calcite             |
| 32  | 0.57  | 40.05 | 0.03            | 0               | 60.79           | 101.43 | calcite, apatite    |
| 33  | 0.55  | 38.83 | 0.06            | 0               | 58.91           | 98.35  | calcite, apatite    |
| 34  | 0.58  | 40.19 | 0.18            | 0               | 60.88           | 101.82 | calcite             |
| 35  | 1.07  | 38.79 | 5.68            | 0               | 54.2            | 99.73  | calcite             |
| 36  | 3.62  | 35.89 | 28.86           | 0               | 31.21           | 99.58  | calcite             |

**2 weeks equilibration,  $\text{PO}_4 = 50 \text{ mmol}\cdot\text{kg}^{-1}$ ,  $\text{F} = 0 \text{ mmol}\cdot\text{kg}^{-1}$**

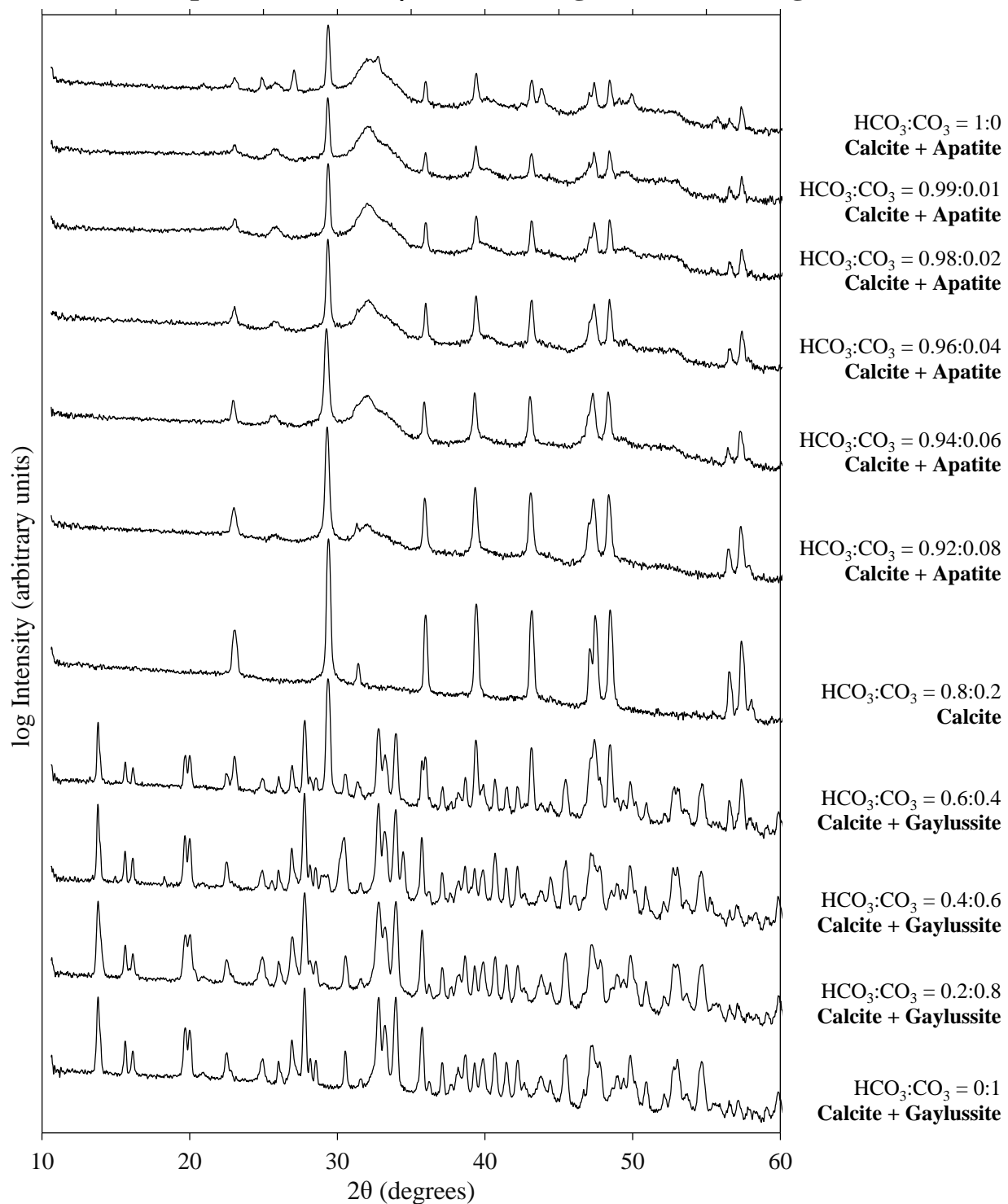


Fig. S2. XRD profiles of saturated carbonate brines containing  $50 \text{ mmol}\cdot\text{kg}^{-1}$  phosphate (no added F) equilibrated for two weeks at various  $\text{HCO}_3:\text{CO}_3$  ratios. This corresponds to sample numbers 1 to 11 in Table S1 and Table S2.



**2 weeks equilibration,  $\text{PO}_4 = 50 \text{ mmol}\cdot\text{kg}^{-1}$ ,  $\text{F} = 10 \text{ mmol}\cdot\text{kg}^{-1}$**

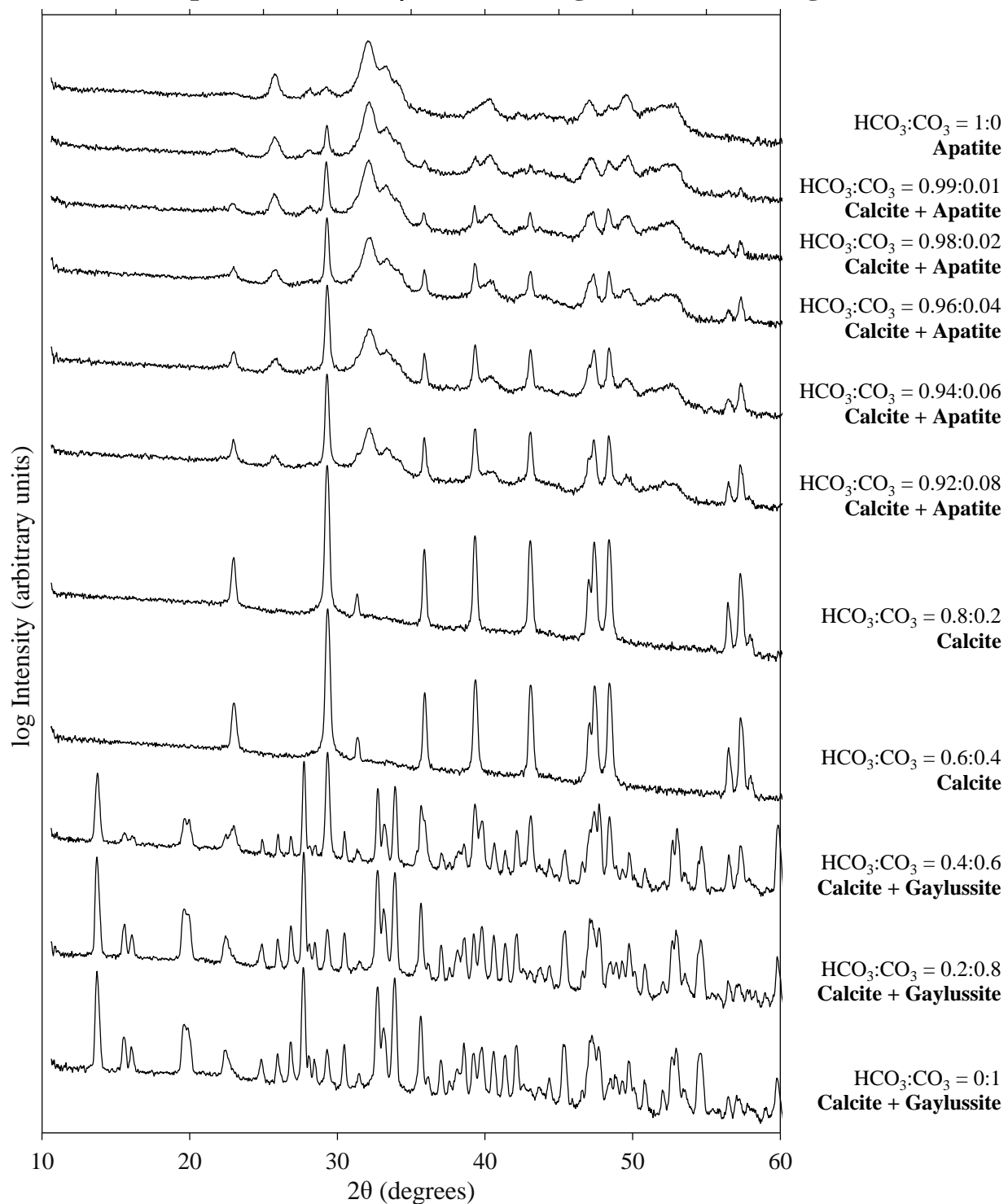


Fig. S3. XRD profiles of saturated carbonate brines containing  $50 \text{ mmol}\cdot\text{kg}^{-1}$  phosphate and  $10 \text{ mmol}\cdot\text{kg}^{-1}$   $\text{F}^-$  equilibrated for two weeks at various molar  $\text{HCO}_3:\text{CO}_3$  ratios. This corresponds to sample numbers 12 to 22 in Table S1 and Table S2.

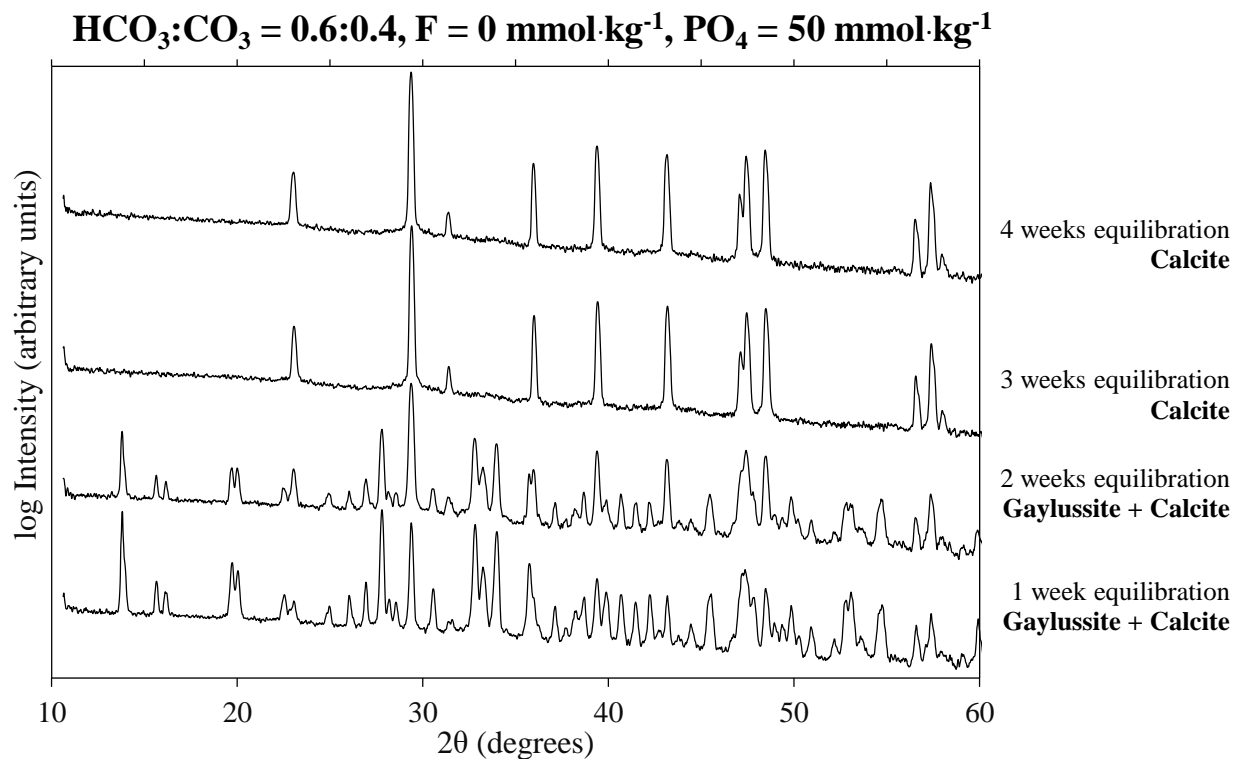


Fig. S4. XRD profiles of saturated carbonate brines with a molar  $\text{HCO}_3:\text{CO}_3$  ratio of 0.6:0.4 (no added  $\text{F}^-$ ) and an initial phosphate concentration of  $50 \text{ mmol}\cdot\text{kg}^{-1}$  equilibrated over one to four weeks. This corresponds to sample numbers 23 to 26 in Table S1 and Table S2.

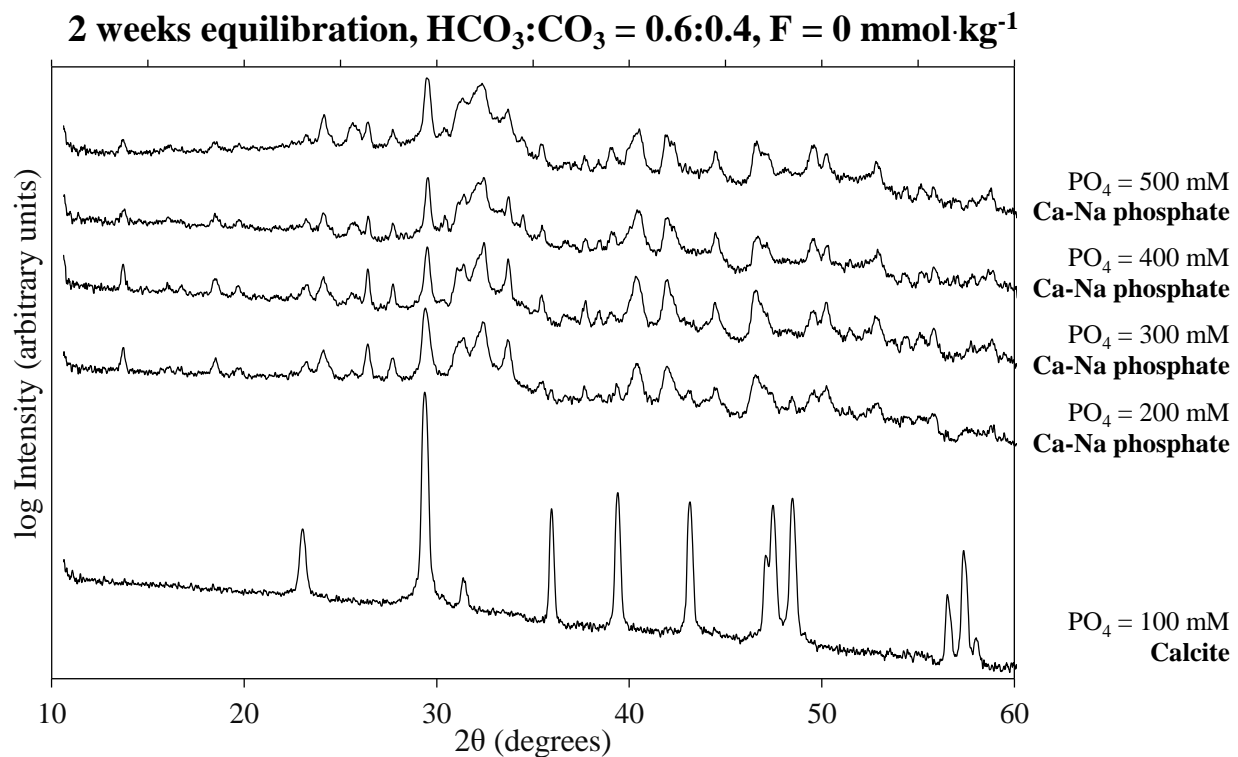


Fig. S5. XRD profiles of saturated carbonate brines with a molar  $\text{HCO}_3^-:\text{CO}_3^{2-}$  ratio of 0.6:0.4 (no added F<sup>-</sup>) equilibrated for two weeks at various initial phosphate concentrations. This corresponds to sample numbers 27 to 31 in Table S1 and Table S2.

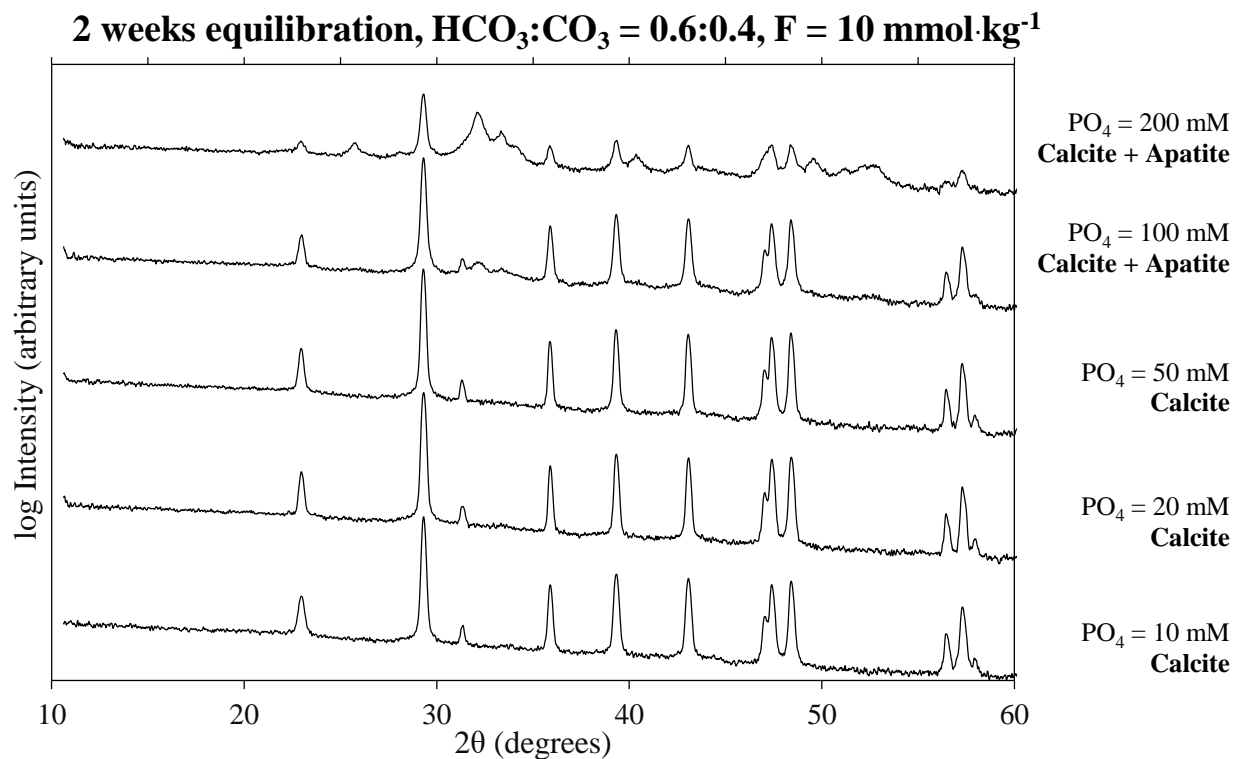


Fig. S6. XRD profiles of saturated carbonate brines with a molar  $\text{HCO}_3:\text{CO}_3$  ratio of 0.6:0.4 and  $10 \text{ mmol}\cdot\text{kg}^{-1} \text{ F}^-$  equilibrated for two weeks at various initial phosphate concentrations. This corresponds to sample numbers 32 to 36 in Table S1 and Table S2.

## Appendix C: Geochemical models

### The Pitzer model

To model concentrated solutions in the Na-Cl-P-CO<sub>2</sub>-H-OH system, we use the Pitzer model (13). The Pitzer equation for the excess Gibbs energy of solution ( $G^{EX}$ ) in a mixed aqueous salt solution containing cations  $c$  and anions  $a$  is given by:

$$(1) \quad G^{EX} = -4A_\phi \ln(1 + b\sqrt{I}) \frac{I}{b} + \sum_c \sum_a m_c m_a (2\beta_{ca} + ZC_{ca}) + \sum_c \sum_{c'} m_c m_{c'} \left( 2\Phi_{cc'} + m_a \sum_a \psi_{cc'a} \right) + \sum_a \sum_{a'} m_a m_{a'} \left( 2\Phi_{aa'} + m_c \sum_c \psi_{aa'c} \right)$$

In this equation, subscript  $M$  indicates a cation, subscript  $X$  indicates an anion,  $c'$  is a cation different from  $c$ ,  $a'$  is an anion different from  $a$ ,  $b$  is a constant ( $1.2 \text{ kg}^{-1/2} \cdot \text{mol}^{-1/2}$ ),  $I$  is the ionic strength given by  $I = \frac{1}{2} \sum m_i z_i^2$ ,  $z_i$  is the ion charge,  $Z$  is given by  $Z = \sum m_i |z_i|$ , and  $A_\phi$  is the Debye–Hückel limiting law slope. Differentiation of  $G^{EX}$  with respect to moles of water ( $n_1$ ) and salt ( $n_i$ ) at molality  $m$  ( $\text{mol} \cdot \text{kg}^{-1}$ ) leads to expressions for the activity coefficients for water ( $a_w$ ) and salt ( $\gamma$ ) respectively:

$$(2) \quad \frac{\partial G^{EX}}{\partial n_1} = RT \ln a_w \quad \text{and} \quad \frac{\partial G^{EX}}{\partial n_i} = RT \ln m_i \gamma_i$$

Importantly, water activities are commonly reported as osmotic coefficients ( $\phi$ ), which are related by the equation:

$$(3) \quad \phi = -55.50844 \frac{\ln a_w}{\sum m_i}$$

The parameters  $\beta$ ,  $C$ , and  $\Phi$  are given by the functions:

$$(4) \quad \beta_{ca} = \beta_{ca}^{(0)} + \beta_{ca}^{(1)} g(\alpha_1 \sqrt{I}) + \beta_{ca}^{(2)} g(\alpha_2 \sqrt{I})$$

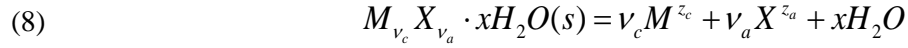
$$(5) \quad C_{ca} = \frac{C_{ca}^\phi}{2\sqrt{|z_c z_a|}}$$

$$(6) \quad \Phi_{ij} = \theta_{ij} + {}^E\theta_{ij}$$

where  ${}^E\theta_{ij}$  is a higher-order electrostatic terms that account for interactions between ions of the same sign, but different charge (i.e.  $z_i \neq z_j$ ), and  $g(x)$  is given by:

$$(7) \quad g(x) = \frac{2[1 - (1+x)e^{-x}]}{x^2}$$

Finally, equilibrium between an aqueous solution and a hydrated salt with  $x$  water molecules,  $\nu_c$  cations, and  $\nu_a$  anions is described by the precipitation/dissolution reaction:



where the thermodynamic equilibrium constant  $K$  for this reaction may be calculated from the ion activity product of the saturated solution:

$$(9) \quad K = (m_c \gamma_c)^{\nu_c} (m_a \gamma_a)^{\nu_a} a_w^x$$

These equations indicate that the Pitzer equations describe properties in mixed electrolyte solutions using the temperature dependent Pitzer parameters  $\beta^{(0)}$ ,  $\beta^{(1)}$ ,  $\beta^{(2)}$ ,  $C^\phi$ ,  $\theta$ , and  $\psi$ , equilibrium constants  $K$ , and temperature-invariant parameters  $\alpha_1$  and  $\alpha_2$ . For Pitzer parameters, PHREEQC uses the temperature dependent expression:

$$(10) \quad P = a_0 + a_1 \left( \frac{1}{T} - \frac{1}{T_r} \right) + a_2 \ln \left( \frac{T}{T_r} \right) + a_3 (T - T_r) + a_4 (T^2 - T_r^2) + a_5 \left( \frac{1}{T^2} - \frac{1}{T_r^2} \right)$$

where  $a_i$  are empirical fitted parameters,  $T_r$  is a reference temperature at 298.15 K, and  $P$  is a Pitzer parameter. For equilibrium constants, PHREEQC uses the temperature dependent expression:

$$(11) \quad \log K = a_1 + a_2 T + \frac{a_3}{T} + a_4 \log T + \frac{a_5}{T^2} + a_6 T^2$$

### ***Fits to experimental data on phosphate solubility***

Experimental data on pure saturated sodium phosphate solutions are taken from Seidel (14), and fit to the Pitzer model described above by least-squares-minimization. The experimental data and the resulting model fits are given in Fig. S7.

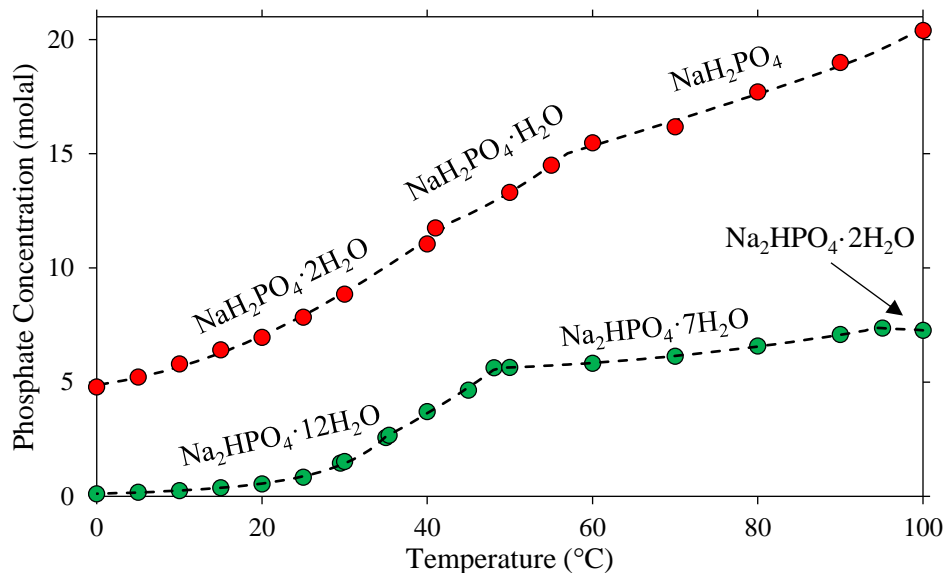


Fig. S7. Experimental solubility measurements (molal) for saturated sodium phosphate solutions at variable temperature for  $\text{NaH}_2\text{PO}_4$  (red circles) and  $\text{Na}_2\text{HPO}_4$  (green circles) salts. The modeled solubility of these salts is given as dashed lines.

### *PHREEQC database file*

The following PHREEQC input code was used to model the solubility of phosphate salts in the Na-Cl-P-CO<sub>2</sub>-H-OH system over a temperature range of 0 to 100°C. The interactive version of PHREEQC is available at <https://www.usgs.gov/software/phreeqc-version-3/>. If using the interactive version of PHREEQC, the definitions of all input parameters given below are well-described in the program. We have commented on the code primarily to specify the source reference for specific parameters.

```
# Parameters for chloride and carbonate salts and CO2 gas are taken from:
# Marion, G. M., et al. (2011).
# Modeling hot spring chemistries with applications to martian silica formation.
# Icarus 212(2): 629–642.

# Parameters for phosphate salts are taken from:
# Scharge, T., et al. (2013).
# Thermodynamic modelling of high salinary phosphate solutions. I. Binary systems.
# The Journal of Chemical Thermodynamics 64: 249-256.
# Scharge, T., et al. (2015).
# Thermodynamic modeling of high salinary phosphate solutions II. Ternary and higher systems.
# The Journal of Chemical Thermodynamics 80: 172-183.
```

```
PITZER
-MacInnes false
-use_etheta true
-redox false
```

```
SOLUTION_MASTER_SPECIES
H H+ -1. H 1.008
H(1) H+ -1. 0.0
E e- 0.0 0.0 0.0
O H2O 0.0 O 15.999
O(-2) H2O 0.0 0.0
Na Na+ 0.0 Na 22.99
Cl Cl- 0.0 Cl 35.45
```

C CO3-2 2.0 HCO3 12.015  
C(4) CO3-2 2.0 HCO3 12.015  
P PO4-3 0 94.973 30.973762  
P(5) PO4-3 0 94.973

SOLUTION\_SPECIES

H+ = H+  
log\_k 0

e- = e-  
log\_k 0

H2O = H2O  
log\_k 0

Na+ = Na+  
log\_k 0

Cl- = Cl-  
log\_k 0

CO3-2 = CO3-2  
log\_k 0

PO4-3 = PO4-3  
log\_k 0

H2O = OH- + H+  
-analytic -2.2219506201E+02 -5.5058066492E-01 -1.4737247297E+04 1.5156364455E+02 7.7093244810E+05 4.2832724439E-04

CO3-2 + H+ = HCO3-  
-analytic 7.8843549125E+01 2.8114156336E-02 -3.5739677566E+03 -2.8384191832E+01 4.7335781578E+05 0

CO3-2 + 2 H+ = CO2 + H2O  
-analytic 3.3245684222E+02 7.3424990888E-02 -1.9829264031E+04 -1.1794430937E+02 1.8387797092E+06 0

2H+ + PO4-3 = H2PO4-  
log\_k 19.562  
-delta\_h -4.520 kcal

3H+ + PO4-3 = H3PO4  
log\_k 21.702  
-delta\_h -10.1 kJ

H+ + PO4-3 = HPO4-2  
log\_k 12.35  
-delta\_h -3.530 kcal

PHASES

Halite # From Marion et al. 2011

NaCl = Cl- + Na+  
-analytic -1.2527916896E+02 -1.5940706427E-01 -7.1582997565E+00 6.6592262608E+01 -7.6881371104E-02 1.0843908037E-04

Na2CO3:7H2O # From Marion et al. 2011

Na2CO3:7H2O = 2Na+ + CO3-2 + 7H2O  
-analytic -1.0242414096E+01 3.2849157355E-02 0 0 0 0

Na2CO3:H2O # From Marion et al. 2011

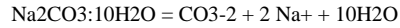
Na2CO3:H2O = 2Na+ + CO3-2 + H2O  
-analytic -2.8774550065E+01 1.8458757574E-01 0 0 0 -2.9016373919E-04

Nahcolite # From Marion et al. 2011

NaHCO3 = HCO3- + Na+  
-analytic 2.7096628475E+02 4.6935820304E-01 1.5642665039E+01 -1.5204447068E+02 1.6854829142E-01 -3.9508831422E-04

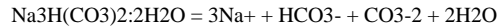


Natron # From Marion et al. 2011



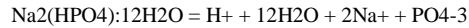
-analytical -5.9688261032E+00 -7.4737824292E-03 0 0 0 8.3268627375E-05

Trona # From Marion et al. 2011



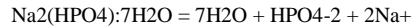
-analytical -1.01750000E+00 1.28307435E-02 -9.59229969E+01 -1.39706624E+00 2.82831158E+03 -8.84486220E-07

$\text{Na}_2(\text{HPO}_4) \cdot 12\text{H}_2\text{O}$  # From this study.



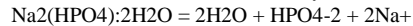
-analytical\_expression -81.310371231 0.39641732552 0 0 0 -0.00057403221891

$\text{Na}_2(\text{HPO}_4) \cdot 7\text{H}_2\text{O}$  # From this study.



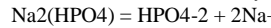
-analytical\_expression -53.300652324 0.31115586643 0 0 0 -0.00046145146621

$\text{Na}_2(\text{HPO}_4) \cdot 2\text{H}_2\text{O}$  # From this study.



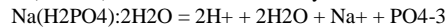
-analytical\_expression 9.7729128374 -0.059178506134 0 0 0 8.4416737735e-05

$\text{Na}_2(\text{HPO}_4)$  # From this study.



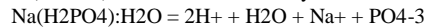
-analytical\_expression 13.896733053 -0.059661090262 0 0 0 5.7293521435e-05

$\text{Na}(\text{H}_2\text{PO}_4) \cdot 2\text{H}_2\text{O}$  # From this study.



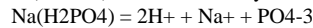
-analytical\_expression -10.856644409 -0.082448426323 0 0 0 0.00018313420267

$\text{Na}(\text{H}_2\text{PO}_4) \cdot \text{H}_2\text{O}$  # From this study.



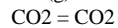
-analytical\_expression 46.342978362 -0.43751747619 0 0 0 0.00073603174603

$\text{Na}(\text{H}_2\text{PO}_4)$  # From this study.



-analytical\_expression -17.735301819 -0.0278227 0 0 0 8.6142857143e-05

$\text{CO}_2(\text{g})$  # From Marion et al. 2011



-analytical 7.6172730397E+01 1.4954581339E-02 -5.1694861624E+03 -2.8759485533E+01 5.6914636107E+05 0.0000000000E+00

PITZER

-B0

# The following are from Marion et al. 2011

$\text{H}^+$  Cl- 1.9794612033E-01 4.3930392007E-02 2.6162364573E-04 -5.3121505493E-04 3.4074178888E-10 -1.3794988905E+00

$\text{Na}^+$  Cl- 7.6273259396E-02 -1.0677687696E+03 -5.2850452529E+00 9.0310652648E-03 -2.5394712901E-06 1.4568462343E+04

$\text{Na}^+$   $\text{CO}_3^{2-}$  3.6204808669E-02 1.1083789213E+03 1.1198570286E+01 -2.3301689083E-02 1.4225931266E-11 -1.0139889781E+01

$\text{Na}^+$   $\text{HCO}_3^-$  2.8002054979E-02 6.8287100127E+02 6.8994999437E+00 -1.4459103667E-02 -1.0139500105E-10 4.8617733194E+00

$\text{Na}^+$  OH- -7.9555220526E-02 2.0309032437E+04 1.6146658627E+02 -5.2616228562E-01 2.9653500975E-04 -5.1829489159E+05

# The following are from Scharge et al. 2013, 2015

$\text{Na}^+$   $\text{H}_2\text{PO}_4^-$  -0.0436

$\text{Na}^+$   $\text{HPO}_4^{2-}$  -0.0172

$\text{Na}^+$   $\text{PO}_4^{3-}$  0.15641

-B1

# The following are from Marion et al. 2011

$\text{H}^+$  Cl- 1.7663995597E-01 -4.4613022946E+04 -3.1259930375E+02 9.5812792829E-01 -5.3080804721E-04 1.2316610809E+06

$\text{Na}^+$  Cl- 2.8041722849E-01 -4.7934459033E+03 -6.9757728955E+01 2.2182662176E-01 -1.0800038619E-04 -3.1269129963E+05

$\text{Na}^+$   $\text{CO}_3^{2-}$  1.5120691287E+00 4.4124805360E+03 4.4581885679E+01 -9.9890728880E-02 -2.3470887122E-10 1.0021144087E+00

$\text{Na}^+$   $\text{HCO}_3^-$  4.4005226296E-02 1.1292842314E+03 1.1410242105E+01 -2.4464729852E-02 -7.4828259687E-02 3.3354784151E+00

$\text{Na}^+$  OH- 2.5311163491E-01 1.4885507672E+04 1.1834672330E+02 -3.9540544436E-01 2.3380756117E-04 -3.7988491809E+05

# The following are from Scharge et al. 2013, 2015

$\text{Na}^+$   $\text{H}_2\text{PO}_4^-$  -0.03389

$\text{Na}^+$   $\text{HPO}_4^{2-}$  1.2116

$\text{Na}^+$   $\text{PO}_4^{3-}$  3.9397

-C0

# The following are from Marion et al. 2011

H+ Cl- -2.8913465588E-03 1.0693004789E-02 5.5410207932E-05 1.7224827506E-05 -5.9323763662E-08 -3.7953644554E-01  
Na+ Cl- 1.2711016441E-03 7.7695148783E+01 2.3007504621E-01 -8.0897946811E-05 -1.1941587694E-07 -2.0177121991E+03  
Na+ CO3-2 0.0052

Na+ OH- 4.1159992172E-03 7.3302950838E+02 5.8279924019E+00 -2.0502290395E-02 1.2873934762E-05 -1.8707050080E+04

# The following are from Scharge et al. 2013, 2015

Na+ H2PO4- 0.00605

Na+ HPO4-2 0.00585

Na+ PO4-3 -0.03498

-LAMDA

# The following are from Marion et al. 2011

Cl- CO2 2.0480415080E-02 -3.3159597997E+04 -3.1582776282E+02 9.9643227553E-01 -5.2121983640E-04 -6.0314596673E-01

Na+ CO2 8.1474353447E-02 1.0939930101E+05 1.0470213325E+03 -3.3265653899E+00 1.7531997031E-03 1.2758007796E+00

-PSI

# The following are from Marion et al. 2011

Cl- CO3-2 Na+ 8.6555626983E-03 -1.1578726767E+01 -1.1401251201E-01 4.4733586264E-04 -4.6816398956E-07 3.7067215792E+02

Cl- HCO3- Na+ -1.2777037089E-02 -1.1975486345E+01 -1.4023338938E-01 5.1084176969E-04 -5.9489945059E-07 4.5438567976E+02

Cl- OH- Na+ -0.006

HCO3- CO3-2 Na+ 0.002

Na+ H+ Cl- -0.0037

OH- CO3-2 Na+ -0.017

# The following are from Scharge et al. 2013, 2015

Cl- H2PO4- Na+ -0.01208

Cl- HPO4-2 Na+ -0.00883

Cl- PO4-3 Na+ -0.00243

HPO4-2 H2PO4- Na+ 0.03781

PO4-3 HPO4-2 Na+ 0.00207

CO3-2 PO4-3 Na+ -0.01449774

-THETA

# The following are from Marion et al. 2011

Cl- CO3-2 -0.02

Cl- HCO3- 0.03

Cl- OH- -0.05

HCO3- CO3-2 -0.04

Na+ H+ 0.036

OH- CO3-2 0.1

# The following are from Scharge et al. 2013, 2015

Cl- H2PO4- 0.10037

Cl- HPO4-2 0.07083

Cl- PO4-3 0.24341

H2PO4- HPO4-2 -0.32361

PO4-3 HPO4-2 0.25528

CO3-2 PO4-3 0.19766089

-ZETA

# The following are from Marion et al. 2011

H+ Cl- CO2 -4.7051879034E-03 1.6334349475E+04 1.5238364378E+02 -4.7047340910E-01 2.4052572265E-04 1.2740734776

Na+ Cl- CO2 -5.7153028547E-04 6.87905500E+03 7.3745255829E+01 -2.58005360E-01 1.4782317370E-04 -7.78048610E-01

-APHI

# The following are from Marion et al. 2011

3.9147193099E-01 3.6897938637E+02 3.5956550857E+00 -1.2908353094E-02 9.5199168775E-06 4.7098725794E+01

### Supplementary References

1. Eugster HP & Jones BF (1979) Behavior of major solutes during closed-basin brine evolution. *American Journal of Science* 279(6):609-631.
2. Smith GI & Stuiver M (1979) Subsurface stratigraphy and geochemistry of late Quaternary evaporites, Searles Lake, California. *Geological Survey Professional Paper* 1043:1-130.
3. Friedman I, Smith GI, & Hardcastle KG (1976) Studies of quaternary saline lakes—II. Isotopic and compositional changes during desiccation of the brines in Owens Lake, California, 1969–1971. *Geochim. Cosmochim. Acta* 40(5):501-511.
4. Felmy AR & Weare JH (1986) The prediction of borate mineral equilibria in natural waters: Application to Searles Lake, California. *Geochim. Cosmochim. Acta* 50(12):2771-2783.
5. Grew ES, Bada JL, & Hazen RM (2011) Borate minerals and origin of the RNA world. *Origins of Life and Evolution of Biospheres* 41(4):307-316.
6. Hirst JF (2013) Sedimentology, diagenesis and hydrochemistry of the saline, alkaline lakes on the Cariboo Plateau, Interior British Columbia, Canada. Ph.D. (University of Saskatchewan, Saskatoon).
7. Clarke FW (1924) The composition of the river and lake waters of the United States. *US Government Printing Office* 135.
8. Felmy AR, Dixon DA, Rustad JR, Mason MJ, & Onishi LM (1998) The hydrolysis and carbonate complexation of strontium and calcium in aqueous solution. Use of molecular modeling calculations in the development of aqueous thermodynamic models. *J. Chem. Thermodyn.* 30(9):1103-1120.
9. Jones BE, Grant WD, Duckworth AW, & Owenson GG (1998) Microbial diversity of soda lakes. *Extremophiles* 2(3):191-200.
10. Eugster HP & Hardie LA (1978) Saline lakes. *Lakes*, (Springer, New York), pp 237-293.
11. Mochizuki A, *et al.* (2018) Distribution of trace elements and the influence of major-ion water chemistry in saline lakes. *Limnology and Oceanography* 63(3):1253-1263.
12. Feldman I (1956) Use and abuse of pH measurements. *Anal. Chem.* 28(12):1859-1866.
13. Pitzer KS (1991) Ion interaction approach: Theory and data correlation. *Activity Coefficients in Electrolyte Solutions*, (CRC Press, Boca Raton), second Ed, pp 75–153.
14. Seidell A (1919) *Solubilities of inorganic and organic compounds* (D. Van Nostrand Company).